Biomedical Sciences and Clinical Medicine 2022;61(4):161-71.
doi:10.12982/BSCM.2022.22
https://www.med.cmu.ac.th/bscm/

BSCM
Biomedical Sciences and Clinical Medicine

Original Article **Open Access**

Clinical Examination and Single-phase Contrast-enhanced CT Scans to Distinguish Benign Lesions from Malignant Tumors of the Parotid Gland

Chakri Madla[1], Salita Angkurawaranon[1], Hanpon Klibngern[2] and Sayanan Chowsilpa[3]

[1]Department of Radiology, [2]Department of Otolaryngology, [3] Department of Pathology, Faculty of Medicine, Chiang Mai University, Chiang Mai, Thailand

Correspondence: Salita Angkurawaranon, MD, Department of Radiology, Faculty of Medicine, Chiang Mai University, Chiang Mai, 50200, Thailand.
E-mail: nook147@gmail.com

Received: May 6, 2022;
Revised: May 20, 2022;
Accepted: May 26, 2022

ABSTRACT

OBJECTIVE To distinguish between benign lesions and malignant tumors of the parotid gland through physical examination and analysis of single-phase contrast-enhanced CT imaging.

METHODS A retrospective study of parotid gland masses in adult patients (age > 15 years) at Maharaj Nakorn Chiang Mai Hospital from 2014 to 2021. Patient demographic data included gender, age and smoking history. Characteristics of parotid masses were established based on physical examinations including mass consistency, pain/tenderness, invasion of surrounding tissue including fixation, skin involvement, trismus and facial nerve palsy, as well as imaging findings indicating mass location, size, number, distribution, shape, margin, composition, extra-parenchymal extension and calcification.

RESULTS A total of 78 patients (10 exhibiting bilateral parotid gland involvement) were diagnosed with a total of 44 benign lesions and 34 malignant tumors. Significant parameters for suspicion of malignancy were determined by two clinical examinations, hard consistency (odds ratio = 60.00, 95% CI = 4.72 to 763.01) and pain/tenderness (odds ratio = 7.45, 95% CI = 1.90 to 29.25) and four imaging findings composed of irregular shape (OR = 7.00, 95% CI = 1.69 to 28.92), ill-defined margins (OR = 10.15, 95% CI = 3.28 to 31.44), extra-parenchymal extension (OR = 32.50, 95% CI = 8.88 to 118.99) and calcification (OR = 6.97, 95% CI = 1.74 to 27.88).

CONCLUSIONS Clinical examination and findings obtained from single-phase contrast-enhanced CT scans can help to distinguish benign from malignant parotid masses.

KEYWORDS parotid gland, computed tomography, pleomorphic adenoma, mucoepidermoid carcinoma

INTRODUCTION

The salivary glands are the site of origin of a wide variety of neoplasms making them a significant challenge for radiologists and clinicians (1). Salivary gland tumors most commonly occur in the parotid gland. For head and neck surgeons, preoperative differentiation between benign and malignant tumors is crucial and can help plan the extent of surgery. For benign or low-grade tumors confined to the superficial lobe of the parotid gland, superficial parotidectomy is the optimal treatment. However, for

large high-grade tumors, the surgeon may have to be prepared for more extensive surgery such as facial nerve sacrifice and neck dissection (2). The degrees of sensitivity and specificity of FNA in distinguishing between benign and malignant neoplasia of the parotid gland are between 33-67% and 100%, respectively (3-5). Surprisingly, sensitivity is generally lower and more variable than specificity. Opponents of physician argue that FNA is unnecessary in most cases owing to an unacceptably high rate of false negatives and a low degree of sensitivity (6-9). They comment that the size and location of the lesion are more influential in the choice of operation than FNA diagnosis. However, the additional information gained from clinical assessments and CT imaging can assist in differentiating between benign and malignant tumors in the parotid gland.

There are certain clues of malignant behavior that can be identified from a patient's history, as well as various signs and symptoms. Both history of heavy smoking and of irradiation in the head and neck area from a young age have been observed to increase the risk of certain types of salivary gland tumors (10,11). The most common presenting symptom of a parotid gland tumor is mass, but this is not indicative of a benign or malignant status. Details of mass characteristics, including consistency, invasion of surrounding tissue by fixation of the mass, skin invasion, facial palsy, trismus, pain or tenderness and enlarged cervical lymph nodes, are considered significantly suggestive of malignancy (12).

Diagnostic imaging also plays an important role in the evaluation of parotid gland tumors. MRI is currently the modality of choice for evaluating salivary gland lesions because its higher soft tissue resolution allows for better identification of internal tumor characteristics (13-15). However, MRI is associated with the disadvantages of limited availability, high cost and the longer time required for treatment. Conversely, CT is considered an extremely efficient imaging technique that has a lower cost, more widely available and has a shorter treatment time. Previous CT imaging-based research studies have usually focused on the pattern enhancement of parotid tumors in an attempt to initiate a dynamic post-contrast study to differentiate between benign and malignant tumors (16-19). However, because many parotid gland lesions are frequently found incidentally for other reasons (20), and a dynamic post-contrast study is often not employed to evaluate the parotid tumors in routine practice. For not conducting a dynamic post-contrast study is radiation dose. Although limiting the field of the delayed scan to the parotid gland, the additional scan still increases the radiation dose to the lens, the most radiosensitive tissue in the human body (21). Radiation-induced cataracts are the issue of greatest concern for patients undergoing head or neck CT examinations. A process of distinguishing between benign and malignant parotid tumors by morphological characteristics from a single-phase post-contrast CT study employing one diagnostic strategy has been developed for identify the diagnosis subtypes of parotid tumors (22).

The objective of this study was to investigate the potential of the patient's signs and symptoms combined with the findings of single-phase contrast-enhanced CT images in distinguishing benign tumors from malignant parotid gland tumors.

METHODS

In this retrospective, descriptive and analytic studies were approved by the research committee of our institute. A list of patients was obtained from the electronic medical resources of the Otolaryngology Department, Maharaj Nakorn Chiang Mai Hospital from 2014 to 2021. The inclusion criteria were age more than 15 years, having parotid mass and having undergone surgery at Maharaj Nakorn Chiang Mai Hospital. The exclusion criteria were poor imaging quality due to motion or severe metallic artifact, non-contrast CT scans, post-excisional imaging, preoperative images with other modalities and no histopathologic documentation after surgery.

Data collection and evaluation

Demographic and clinical data

Data pertaining to age, gender, history of smoking plus mass characteristics including consistency, pain or tenderness, invasion of surrounding tissue comprised of fixation, skin involvement, trismus, facial nerve palsy and

the final histopathology were obtained from electronic medical records.

CT Imaging

CT scans were performed using a 16-slice Toshiba Aquilion MDCT(Tochigi-Ken, Japan), 64-slice Siemens Definition MDCT (Forchheim, Germany) or a 192-slice Siemens Definition DSCT (Forchheim, Germany) at 1-mm slice thickness. Non-contrast CT scans covering the parotid area were performed. Subsequently, 70-mL of intravenous iodinated contrast media was administered to each patient at an injection contrast rate of 2.5-3 mL/sec. Contrast-enhanced images covering the parotid gland and neck region were then obtained 80 seconds after contrast administration.

The collected imaging findings included the following: (1) location of the parotid mass, the deep lobe and/or the superficial lobe using a stylomandibular tunnel (a line between the mandibular ramus and the styloid process), (2) size (maximal axial dimension in centimeters, (3) number of masses (single or multiple), (4) distribution of masses (unilateral or bilateral), (5) shape of masses (round/oval, lobulated or irregular), (6) margins (sharp or ill-defined), (7) composition of the masses (entirely cystic mass, entirely cystic mass with a peripheral enhancing rim, solid and cystic mass with a large cystic portion, mainly solid mass with small cysts or entirely solid enhancing mass), (8) calcification (present or absent within the parotid mass on non-contrast CT), (9) lymphadenopathy (presence or absence of ≥ 5 mm long axis of intra-parotid and peri-parotid node), (10) extra-parenchymal extension (EPE) (presence or absence of the infiltrative tumor in the subcutaneous tissue, skin, masticator space, external ear canal, internal carotid artery or surrounding bone destruction (mandible, mastoid and pterygoid bones).

All of the CT imaging studies were reviewed by two board-certified neurologic diagnostic radiologists and a consensus was reached without disclosure of clinical information or final diagnosis.

Statistical analysis

All data were statistically analyzed using STATA version 15.0. Continuous variables (age and tumor size) are presented as mean and standard deviation (SD) values, while categorical variables are presented as count and percent. Baseline characteristics (mean age, gender and smoking history) were analyzed by bivariate analysis. Correlations between signs and symptoms and imaging findings of malignant tumors were analyzed by Fischer's exact test to establish categorical variables and by the Mann–Whitney U test to establish continuous variables. Logistic regression analysis was used to identify significant signs, symptoms and imaging findings which could potentially facilitate diagnosis of malignant tumors. Statistical significance was defined as a $p < 0.05$. The odds ratios (OR) and 95% confidence intervals are presented as results.

RESULTS

A total of 84 patients presenting with parotid masses were identified from the electronic medical database of the Otolaryngology Department. After exclusions, the final number of patients was 78 (10 patients exhibited bilateral parotid involvement). Among these, there were 44 cases of benign lesions (24 pleomorphic adenomas, 16 Warthin's tumors, 2 with Kimura's disease, 1 monomorphic/basal cell adenoma and 1 oncocytoma) and 34 cases of malignant tumors (11 mucoepidermoid carcinomas, 5 acinic cell carcinomas, 4 carcinoma ex-pleomorphic adenomas, 4 salivary duct carcinomas, 3 lymphoepithelial carcinomas, 3 lymphomas, 2 adenoid cystic carcinomas, 1 hybrid of myoepithelial and acinic cell carcinoma and 1 metastasis squamous cell carcinoma of the nasopharynx).

Demographic data

The mean age of the participating subjects was 53.53 years (range 15 to 85 years) with 53% male and 47% female participants. There were 44 benign lesions and 34 malignant tumors. Approximately 37% of the patents had a history of smoking. A summary of the patients' characteristics is shown in Table 1. No statistically significant differences in the demographic data were observed between benign lesions and malignant tumors.

Clinical examination and Imaging findings

Clinical parameters and imaging findings that revealed statistically significant differences

Table 1. Demographic data of patients with parotid masses

Variables	All patients (N=78)	Benign lesion (N=44)	Malignant tumor (N=34)	*p*-value[a]
Gender				0.953
Male	41 (52.6)	23 (52.3)	18 (52.9)	
Female	37 (47.4)	21 (47.7)	16 (47.1)	
Age				0.519[#]
Mean±SD	53.53±16.79	54.34±15.67	52.47±18.33	
Smoking				0.438
No	49 (62.8)	26 (59.1)	23 (67.6)	
Yes	29 (37.2)	18 (40.9)	11 (32.4)	

[a]Chi-square test was used for analysis of categorical data; [#]*P*-value from Mann–Whitney U test

between benign lesions and malignant tumors included mass consistency, pain/tenderness, facial nerve palsy, invasion of adjacent structures and number of lesions as well as lesion shape, margin, composition, extra-parenchymal extension and calcification.

In terms of the clinical parameters (Table 2), firmness was the most common type of mass consistency (67.9%), with 73% in benign lesions and 62% in malignant tumors. A hard consistency was more frequently found in the malignant tumors of 12 patients (15.38%), but only 2 patients (4.6%) with hard consistency tumors were diagnosed with benign lesions. Masses with a hard consistency are associated with an approximately 60 times greater risk of malignancy than masses with a soft/cystic consistency (odds ratio = 60.00, 95% CI = 4.72 to 763.01). Cystic consistency was more prevalent in benign lesions than in malignant tumors in a case-ratio of 8:1.

Thirty five percent of malignant tumors produced pain or tenderness in patients when compared with 6.8% of benign masses (p = 0.002). Additionally, patients who complained of pain had a 7.5-times greater risk of malignancy than patients that had not complained of pain or tenderness (odds ratio = 7.45, 95% CI = 1.90 to 29.25).

Facial nerve palsy was observed in only three cases of malignant tumors (8.8%), while none of the benign masses were associated with facial palsy (p = 0.044).

Invasion of adjacent structures was observed in 11 cases of malignant tumors (32.4%) but was not observed in any benign lesion cases (p < 0.001).

With regard to the imaging findings (Table 3), there were more multiple lesions in benign masses (8 cases, 18.2%) than in malignant tumors (1 case, 2.9%), while a single mass was observed in 81.8% of cases of benign masses

Table 2. Comparison of signs and symptoms for benign lesions and malignant tumors

Variables	Benign lesion (N=44)	Malignant tumor (N=34)	*p*-value[a]
Consistency			0.001*
Firm	32 (72.7)	21 (61.8)	
Soft	2 (4.6)	0	
Hard	2 (4.6)	12 (35.3)	
Cyst	8 (18.2)	1 (2.9)	
Pain/tender			0.002*
No	41 (93.2)	22 (64.7)	
Yes	3 (6.8)	12 (35.3)	
Facial nerve palsy			0.044*
No	44 (100.0)	31 (91.2)	
Yes	0	3 (8.8)	
Adjacent structures invasion			< 0.001*
No	44 (100.0)	23 (67.6)	
Yes	0	11 (32.4)	

[a]Chi-square test was used for analysis of categorical data and Fisher exact test was used to adjust results with less than five observations for analysis of categorical data.
*Significantly different

Table 3. Comparison of imaging findings for benign lesions and malignant tumors

Variables	Benign lesion (N=44)	Malignant tumor (N=34)	*p*-value[a]
Location			0.361
Superficial	35 (79.5)	24 (70.6)	
Superficial and deep	9 (20.5)	10 (29.4)	
Size			0.217[#]
Mean ± SD	3.19±1.28	3.45±1.22	
Number of tumors			0.037*
Single	36 (81.8)	33 (97.1)	
Multiple	8 (18.2)	1 (2.9)	
Distribution			0.101
Unilateral	38 (86.4)	33 (97.1)	
Bilateral	6 (13.6)	1 (2.9)	
Shape			0.012*
Oval/round	14 (31.8)	3 (8.8)	
Lobulated	16 (36.4)	10 (29.4)	
Irregular	14 (31.8)	21 (61.8)	
Margin			< 0.0001*
Sharp	28 (63.6)	5 (14.7)	
Ill-defined	16 (36.4)	29 (85.3)	
Composition			0.047*
Cystic mass with peripheral enhancement	6 (13.6)	1 (2.9)	
Solid mass with large cystic portion	11 (25.0)	3 (8.8)	
Mainly solid mass with small cysts	13 (29.6)	18 (52.9)	
Entirely solid enhancing mass	14 (31.8)	12 (35.3)	
Lymphadenopathy			0.087
Absent	37 (84.1)	23 (67.6)	
Present	7 (15.9)	11 (32.4)	
EPE			< 0.0001*
Absent	40 (90.9)	8 (23.5)	
Present	4 (9.1)	26 (76.5)	
Calcification (n=73)[b]			0.002*
Absent	39 (92.9)	20 (64.5)	
Present	3 (7.1)	11 (35.5)	

[a]Chi-square test was used for analysis of categorical data, Fisher exact test was used to adjust results with less than 5 observations for analysis of categorical data.
[#]P-value from Mann–Whitney U test; [b]Calcification was evaluated in 73 parotid masses which had undergone non-contrast CT scanning; *Significant difference

and in 97.1% of cases of malignant tumors. The number of lesions showed no statistically significant differences in logistic regression analysis (p = 0.07) (Figure 1).

The shape of the mass was also associated with statistically significant differences (p = 0.012). Malignant tumors exhibited a higher incidence of irregular shapes: 21 cases (61.8%) compared with 14 cases (31.8%) in benign lesions. Benign lesions were associated with a similar proportion of all three tumor shapes (oval/round 31.8%: lobulated 36.4%: irregular 31.8%). According to univariable logistic regression analysis, an irregular shape tumor was indicative of a 7 times higher risk for malignancy than oval/round shape tumors (OR = 7.00, 95% CI= 1.69 to 28.92) (Figure 2A).

Ill-defined margins were more prevalent in malignant tumors (about 85.3% compared with 14.7% of those with sharp tumor margins), while the ratio for benign lesions was 63.6% for sharp margins and 36.4% for ill-defined margins. Ill-defined margins were associated with about a 10 times greater risk of the presence of a malignant tumor compared with sharp margins (OR = 10.15, 95% CI = 3.28 to 31.44).

The tumor composition of malignant tumors and benign lesions showed a significant incidence of either entirely or mainly solid composition of about 88.2 % and 61.4%, respectively. Cystic masses with peripheral enhancement and solid masses with large cystic portions tended to be present in higher numbers in benign lesions than in malignant tumors (17:4 cases).

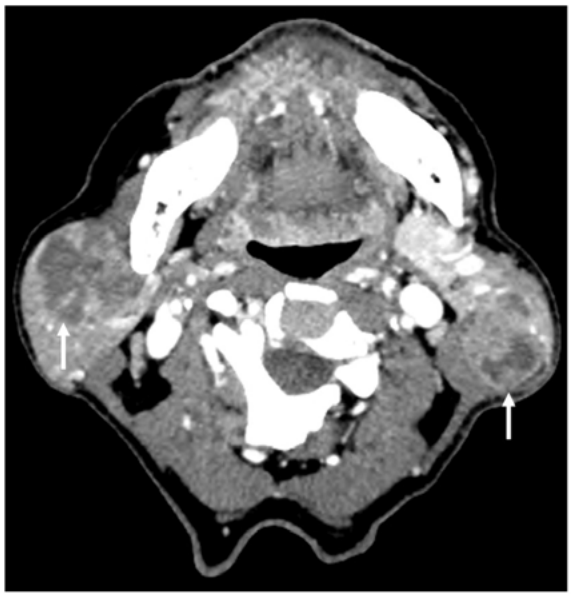

Figure 1. Multiple well-defined solid masses with large cystic portions (arrows) in the tail of the bilateral parotid glands determined to be Warthin's tumor.

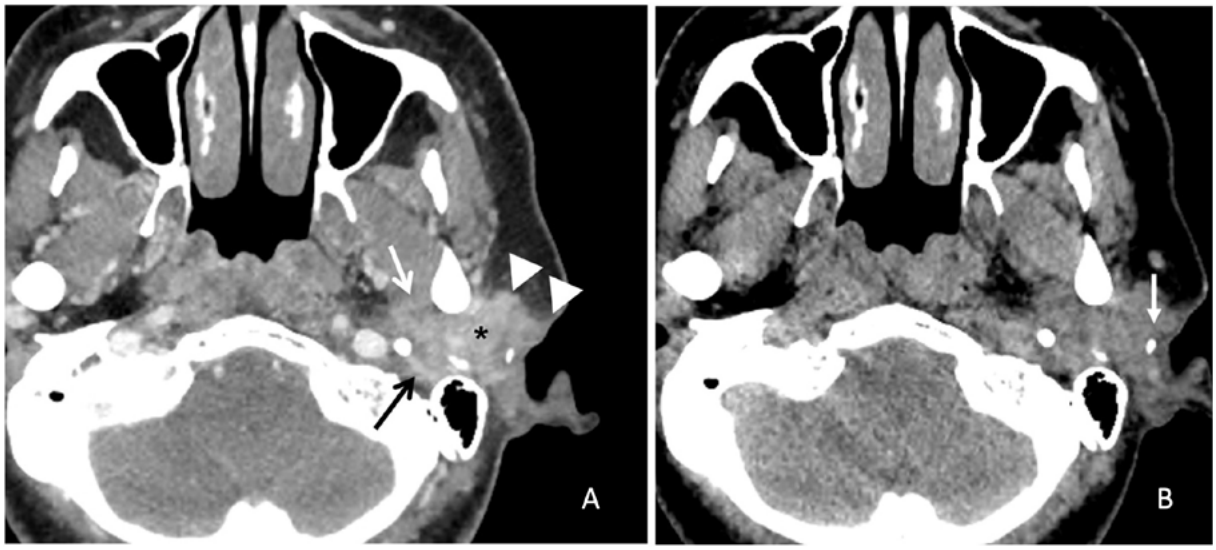

Figure 2. (A) Axial contrast-enhanced CT scan showing an irregular shaped (*), ill-defined margin (black arrow) mass in the left parotid gland with EPE into the subcutaneous tissue and skin (arrowheads) and the medial pterygoid muscle (white arrow). (B) Axial non-contrast CT scan showing intra-tumoral calcification (arrow) determined to be mucoepidermoid carcinoma

EPE was also associated with a significant difference between benign and malignant outcomes with 76.5% in malignant tumors and 9.1% in benign lesions. Masses with EPE were associated with a greater risk of malignant tumors of approximately 32 times that of those without EPE (OR = 32.50, 95% CI = 8.88 to 118.99) (Figure 2A).

Tumor calcification was evaluated in only 73 of 78 patients due to limited access to non-contrast CT scanning. The presence of intra-tumoral calcification was more common in malignant tumors (35.5%) than benign lesions (7.1%). Accordingly, there was a 7 times greater risk for the presence of a malignant tumor in these patients when compared with patients with masses without calcification (OR = 6.97, 95% CI = 1.74 to 27.88) (Figure 2B).

There were no statistically significant differences in terms of location, size, distribution of masses or presented of enlarged cervical lymph nodes.

Binary logistic regression analysis indicated that statistically significant parameters related to malignant parotid tumors include hard consistency, pain or tenderness at the mass, irregular shape, ill-defined margins, extra-parenchymal extension and tumor calcification (Table 4).

Table 4. Signs and symptoms plus imaging findings associated with malignant tumors using binary logistic regression

Factors		*p*-value
Consistency		
Hard	60.00 (4.72, 763.01)	0.002*
Firm	6.56 (0.78, 55.11)	0.08
Soft/cyst	Reference	
Pain/tender		
Present	7.45 (1.90, 29.25)	0.004*
Absent	Reference	
Number		
Single	7.33 (0.87, 61.82)	0.07
Multiple	Reference	
Shape		
Irregular	7.0 (1.70, 28.92)	0.007*
Lobulated	2.92 (6.07, 12.76)	0.15
Oval/round	Reference	
Margin		
Ill-defined	10.15 (3.28, 31.44)	< 0.0001*
Sharp	Reference	
Composition		
Mainly solid mass with small cysts	8.31 (0.89, 77.57)	0.06*
Entirely solid enhancing mass	5.14 (0.54, 48.94)	0.15
Solid mass with a large cystic portion	1.64 (0.14, 19.39)	0.70
Cystic mass with peripheral enhancement	Reference	
EPE		
Present	32.50 (8.88, 118.99)	< 0.0001*
Absent	Reference	
Calcification (n=73)[b]		
Present	6.97 (1.74, 27.88)	0.006*
Absent	Reference	

95% CI, 95% Confidence interval; *p*-value from Wald Statistics test; *, Significant differences; [b]Calcification was evaluated in 73 parotid masses which had undergone non-contrast CT scanning.

DISCUSSION

Our study found that 43.6 % of subjects exhibited malignancies in focal parotid lesions, which was slightly higher than in prior reports (30%) (23,24). This difference may be due to two reasons. First, our study included only surgically proven parotid masses, thus some benign lesions which received conservative treatment were excluded. Second, our hospital is the referral center for the region, so the referral pattern may have resulted in a higher prevalence of malignant parotid tumors.

Our study was designed to employ clinical examination and contrast-enhanced CT scanning without conducting a dynamic study to differentiate between benign lesions and malignant tumors. The significant clinical and imaging parameters related to malignant tumors in our study were comprised of hard consistency, pain or tenderness, irregular shapes, ill-defined margins, extra-parenchymal extension and the presence of tumor calcification.

Pain or tenderness was observed in 35.3% of malignant tumors in our study. This figure is similar to what was observed in a study conducted by Colevas et al. (25) which reported a rate of 33.1%. It has been previously determined that pain and facial paresis are predictive for the presence of perineural invasion in malignant tumors had significantly associated with advanced T and N stages in AJCC TNM tumor staging, high-risk pathologic types, positive margins, and angiolymphatic invasion (26). In previous studies, the majority of cases that involved pain (approximately 82.6%) were associated with adenoid cystic carcinoma (27-29). This contrasts with the outcomes of our study which found that pain was predominantly found in incidences of mucoepidermoid carcinoma (5 out of 12 cases with pain/tenderness).

Our result may be attributed to the small number of adenoid cystic carcinoma cases in our study (2 cases). However, all subjects in this study had experienced symptoms of pain/tenderness. In our study, when pain/tenderness was present in patients with parotid masses, the masses had a 7.4 times greater risk of being a malignant tumor when compared to those without. On the other hand, 7.9% (29) of patients with benign parotid lesions may have experienced some form of pleomorphic adenoma or Warthin's tumor. Our study reported a similar incidence of the association between benign lesions and pain of around 6.8% (3 cases). These lesions included two cases of pleomorphic adenoma and one of Warthin's tumor.

The consistency of the mass is significantly different between benign lesions and malignant tumors (p = 0.001). Masses with a hard consistency are associated with a greater risk of malignancy of approximately 60 times that of masses of soft/cystic consistency. In our study, hard consistency was in concordance with the composition of tumors observed on CT images. All tumors with hard consistency (14 cases) displayed an imaging pattern of an entirely solid enhancing mass and a mainly solid mass with small cysts; in 12 of the 14 cases there was malignancy. Conversely, a cystic and soft consistency tended to occur in more frequently in benign lesions than in malignant tumors (10:1 cases), but the tumor composition varied presented in four distinct patterns. Tumor composition also showed significant differences between benign and malignant tumors (p = 0.047). The pattern that was most likely to appear in a malignancy was mainly a solid mass with small cysts. This outcome was determined to be not quite statistically significant in the logistic regression analysis (p = 0.06). The small cystic area could represent a cystic component or necrosis that was present in our histopathologic study when the carcinoma transformed to a higher grade (30).

Ill-defined margins indicated statistically significant differences between benign and malignant tumors ($p < 0.0001$). Ill-defined margins have been described as the single best tool for discriminating between benign and malignant tumors using post-contrast T1-weighted sequences with fat suppression on MRI (13), with 59% observed in malignant tumors and 21% in benign tumors. In our routine practice, we use contrast-enhanced CT scans as the modality of choice because it is inexpensive, efficient, more readily available, and easy to assess. CT scans can be associated with lower degrees of soft tissue contrast in depicting the sharpness of tumor margins because there is little difference between tumor and normal parotid gland attenuation. Accordingly, this can mislead radiologists to interpret the margins of the mass as ill-defined. Thus, our results related to CT images revealed a relatively high percentage of ill-defined margins in both benign lesions and malignant tumors of 36.4% and 85.3%, respectively.

In cases of more aggressive carcinoma, the tumor margin is typically more ill-defined and un-encapsulated (31) indicating that the shape of the tumor is irregular. We found irregular shapes in approximately 61.8% of malignant tumors and 31.8% of benign lesions. This type of shape has been reported in about 16% of malignant tumors examined by MRI, whereas none of the benign lesions were classified as having an irregular shape (14). One reason for the differences in the number of tumors exhibiting this shape is associated with the definition of "irregular shape". Identification of an irregular shape in parotid tumor imaging is somewhat controversial because sometimes the tumor material is overlapping resulting in a lobulated shape (32). Moreover, many authors have focused on the point that the tumor margin is more reliable than the shape (33) thus these terms would not be clarified.

EPE is defined by the extension of the tumor into adjacent soft tissue, skin, masticator space, and/or bone. It has been suggested that such an extension can identify malignant tumors with a degree of accuracy 154 times greater than for tumors without extension. In this study, there were 4 cases (9.1%) of benign lesions with EPE. This is in contrast with a previous study (14) which reported that none of the benign lesions exhibited EPE. The 4 cases were comprised of two cases of Kimura's disease and one each of Warthin's tumor and pleomorphic adenoma. Kimura's disease is a chronic inflammatory

disease. Previous studies (34,35) have reported ill-defined margins in about 98% and an EPE in around 93% of cases with those diseases. Lymph node involvement associated with Kimura's disease can cause radiologists to misdiagnose metastatic lymph nodes as malignant parotid tumors. Warthin's tumor is a benign tumor that can mimic malignancy due to the presence of lesions in the periparotid region (36) which can be interpreted as an EPE. However, male gender, heavy smoking, and multiple lesions or bilateral parotid involvement are significant clues that can be used to indicate the presence of Warthin's tumor (36-38).

A prior systematic review (39) reported that calcification was found in 47.5% of malignant salivary gland tumors, in 25.0% of benign tumors and in 27.5% of the malignant transformations of benign tumors. This is in contrast with the findings of a study conducted by Jin et al. (16) which reported that calcifications were present only in some incidences of pleomorphic adenoma. In our study, calcification was found in both malignant tumors and in benign lesions at 35.5% (11 cases) and 7.1% (3 cases), respectively. Mucoepidermoid carcinoma was associated with the highest degree of calcification in 4 out of 11 malignancy cases. Some authors have proposed that calcifications are associated with the incidence of high-grade malignancy (40,41), but the findings of another recent study argue that calcification can be unrelated to tumor grade (42) as is the case in our study. Additionally, as has also been reported in previously published studies (16,39), our study determined that calcification can be associated with incidences of pleomorphic adenoma (2 of 24 cases) and their malignant transformation into carcinoma ex-pleomorphic adenomas (3 of 4 cases). Intra-tumoral calcifications in pleomorphic adenomas are presumed to be related to the ossification of cartilage structure within the tumor (39,43).

Our study did have some important limitations. First, different terms were at times used for clinical assessments that were accomplished without a standardized approach as in previous retrospective studies. Second, some cytologically proven benign parotid tumors that were diagnosed without surgical intervention or which were associated with unresectable carcinoma were excluded from our study. A prospective study to compare single phase and multiphase contrast enhanced CT scans of the parotid gland including consideration of radiation dose to the lenses should be investigated in the future.

CONCLUSIONS

Clinical assessment and single-phase contrast CT scans can be used in preoperative assessments for differentiating benign and malignant tumors without using dynamic contrast imaging. Statistically significant parameters for malignancy include pain or tenderness, irregular shape, ill-defined margins, extra-parenchymal extension and intra-tumoral calcification.

ACKNOWLEDGMENTS

None

FUNDING

None

CONFLICTS OF INTEREST

None

ADDITIONAL INFORMATION

Author contributions

- C.M. and S.A. conceived the original idea and discussed with K.H. All authors discussed and agreed with the objective and idea of this paper.
- All data was collected by H.K., cleaned up by C.M. and interpretation by C.M. and S.A.
- The main text of the paper was written by C.M. and the clinical examination part was improved by H.K. and the imaging finding part was approved by S.A.
- The presenting data was created by C.M.

REFERENCES

1. Bobati SS, Patil BV, Dombale VD. Histopathological study of salivary gland tumors. J Oral Maxillofac Pathol. 2017;21:46-50.
2. Zuo H. The Clinical Characteristics and CT Findings of Parotid and Submandibular Gland Tumours. J Oncol. 2021;2021:8874100.
3. Al-Khafaji BM, Nestok BR, Katz RL. Fine-needle aspiration of 154 parotid masses with histologic correlation: ten-year experience at the University of Texas M. D. Anderson Cancer Center. Cancer. 1998;84:153-9.

4. Atula T, Greénman R, Laippala P, Klemi PJ. Fine-needle aspiration biopsy in the diagnosis of parotid gland lesions: evaluation of 438 biopsies. Diagn Cytopathol. 1996;15:185-90.
5. Que Hee CG, Perry CF. Fine-needle aspiration cytology of parotid tumours: is it useful? ANZ J Surg. 2001;71:345-8.
6. Hughes JH, Volk EE, Wilbur DC. Pitfalls in salivary gland fine-needle aspiration cytology: lessons from the College of American Pathologists Interlaboratory Comparison Program in Nongynecologic Cytology. Arch Pathol Lab Med. 2005;129:26-31.
7. McGurk M, Hussain K. Role of fine needle aspiration cytology in the management of the discrete parotid lump. Ann R Coll Surg Engl. 1997;79:198-202.
8. Tandon S, Shahab R, Benton JI, Ghosh SK, Sheard J, Jones TM. Fine-needle aspiration cytology in a regional head and neck cancer center: comparison with a systematic review and meta-analysis. Head Neck. 2008;30:1246-52.
9. Tew S, Poole AG, Philips J. Fine-needle aspiration biopsy of parotid lesions: comparison with frozen section. Aust N Z J Surg. 1997;67:438-41.
10. Gill S, Mohan A, Aggarwal S, Varshney A. Mucoepidermoid carcinoma of hard palate. Indian Journal of Pathology and Microbiology. 2018;61:397-8.
11. de Ru JA, Plantinga RF, Majoor MH, van Benthem PP, Slootweg PJ, Peeters PH, et al. Warthin's tumour and smoking. B-ent. 2005;1:63-6.
12. Stodulski D, Mikaszewski B, Stankiewicz C. Signs and symptoms of parotid gland carcinoma and their prognostic value. Int J Oral Maxillofac Surg. 2012;41:801-6.
13. Christe A, Waldherr C, Hallett R, Zbaeren P, Thoeny H. MR imaging of parotid tumors: typical lesion characteristics in MR imaging improve discrimination between benign and malignant disease. AJNR Am J Neuroradiol. 2011;32:1202-7.
14. Tartaglione T, Botto A, Sciandra M, Gaudino S, Danieli L, Parrilla C, et al. Differential diagnosis of parotid gland tumours: which magnetic resonance findings should be taken in account? Acta Otorhinolaryngol Ital. 2015;35:314-20.
15. Yabuuchi H, Fukuya T, Tajima T, Hachitanda Y, Tomita K, Koga M. Salivary gland tumors: diagnostic value of gadolinium-enhanced dynamic MR imaging with histopathologic correlation. Radiology. 2003;226:345-54.
16. Jin GQ, Su DK, Xie D, Zhao W, Liu LD, Zhu XN. Distinguishing benign from malignant parotid gland tumours: low-dose multi-phasic CT protocol with 5-minute delay. Eur Radiol. 2011;21:1692-8.
17. Jung YJ, Han M, Ha EJ, Choi JW. Differentiation of salivary gland tumors through tumor heterogeneity: a comparison between pleomorphic adenoma and Warthin tumor using CT texture analysis. Neuroradiology. 2020;62:1451-8.
18. Kim TY, Lee Y. Contrast-enhanced Multi-detector CT Examination of Parotid Gland Tumors: Determination of the Most Helpful Scanning Delay for Predicting Histologic Subtypes. J Belg Soc Radiol. 2019;103:2.
19. Yerli H, Aydin E, Coskun M, Geyik E, Ozluoglu LN, Haberal N, et al. Dynamic multislice computed tomography findings for parotid gland tumors. J Comput Assist Tomogr. 2007;31:309-16.
20. Kessler AT, Bhatt AA. Review of the Major and Minor Salivary Glands, Part 1: Anatomy, Infectious, and Inflammatory Processes. J Clin Imaging Sci. 2018;8:47.
21. Mosher EG, Butman JA, Folio LR, Biassou NM, Lee C. Lens Dose Reduction by Patient Posture Modification During Neck CT. AJR Am J Roentgenol. 2018;210:1111-7.
22. Xu ZF, Yong F, Yu T, Chen YY, Gao Q, Zhou T, et al. Different histological subtypes of parotid gland tumors: CT findings and diagnostic strategy. World J Radiol. 2013;5:313-20.
23. Bialek EJ, Jakubowski W, Zajkowski P, Szopinski KT, Osmolski A. US of the major salivary glands: anatomy and spatial relationships, pathologic conditions, and pitfalls. Radiographics. 2006;26:745-63.
24. Renehan A, Gleave EN, Hancock BD, Smith P, McGurk M. Long-term follow-up of over 1000 patients with salivary gland tumours treated in a single centre. Br J Surg. 1996;83:1750-4.
25. Colevas S, Thompson J, Glazer T, Hartig G. Prognostic Significance of Pain in Parotid Gland Malignancy. Laryngoscope. 2021;131:1503-8.
26. Huyett P, Duvvuri U, Ferris RL, Johnson JT, Schaitkin BM, Kim S. Perineural Invasion in Parotid Gland Malignancies. Otolaryngol Head Neck Surg. 2018;158:1035-41.
27. Vander Poorten VL, Balm AJ, Hilgers FJ, Tan IB, Loftus-Coll BM, Keus RB, et al. The development of a prognostic score for patients with parotid carcinoma. Cancer. 1999;85:2057-67.
28. Coca-Pelaz A, Rodrigo JP, Bradley PJ, Vander Poorten V, Triantafyllou A, Hunt JL, et al. Adenoid cystic carcinoma of the head and neck-An update. Oral Oncol. 2015;51:652-61.
29. Inaka Y, Kawata R, Haginomori SI, Terada T, Higashino M, Omura S, et al. Symptoms and signs of parotid tumors and their value for diagnosis and prognosis: a 20-year review at a single institution. Int J Clin Oncol. 2021;26:1170-8.
30. Zarbo RJ. Salivary gland neoplasia: a review for the practicing pathologist. Mod Pathol. 2002;15:298-323.
31. Peraza A, Gómez R, Beltran J, Amarista FJ. Mucoepidermoid carcinoma. An update and review of the literature. J Stomatol Oral Maxillofac Surg. 2020;121:713-20.
32. Rzepakowska A, Osuch-Wójcikiewicz E, Sobol M, Cruz R, Sielska-Badurek E, Niemczyk K. The differential diagnosis of parotid gland tumors with

high-resolution ultrasound in otolaryngological practice. Eur Arch Otorhinolaryngol. 2017;274: 3231-40.
33. Gritzmann N, Rettenbacher T, Hollerweger A, Macheiner P, Hübner E. Sonography of the salivary glands. Eur Radiol. 2003;13:964-75.
34. Park SW, Kim HJ, Sung KJ, Lee JH, Park IS. Kimura disease: CT and MR imaging findings. AJNR Am J Neuroradiol. 2012;33:784-8.
35. Zhang R, Ban XH, Mo YX, Lv MM, Duan XH, Shen J, et al. Kimura's disease: the CT and MRI characteristics in fifteen cases. Eur J Radiol. 2011;80:489-97.
36. Ikeda M, Motoori K, Hanazawa T, Nagai Y, Yamamoto S, Ueda T, et al. Warthin tumor of the parotid gland: diagnostic value of MR imaging with histopathologic correlation. AJNR Am J Neuroradiol. 2004;25:1256-62.
37. Wang CW, Chu YH, Chiu DY, Shin N, Hsu HH, Lee JC, et al. JOURNAL CLUB: The Warthin Tumor Score: A Simple and Reliable Method to Distinguish Warthin Tumors From Pleomorphic Adenomas and Carcinomas. AJR Am J Roentgenol. 2018;210:1330-7.
38. Yu Y, Zhang WB, Soh HY, Sun ZP, Yu GY, Peng X. Efficacy of computed tomography features in the differentiation of basal cell adenoma and Warthin tumor in the parotid gland. Oral Surg Oral Med Oral Pathol Oral Radiol. 2021;132:589-96.
39. Farid MM, Farid FM, Hamed WM. Intra-tumoral salivary gland calcification: A systematic review. Egyptian Dental Journal. 2015;61:4936-5204.
40. Rabinov JD. Imaging of salivary gland pathology. Radiol Clin North Am. 2000;38:1047-57, x-xi.
41. Kurabayashi T, Ida M, Yoshino N, Sasaki T, Ishii J, Ueda M. Differential diagnosis of tumours of the minor salivary glands of the palate by computed tomography. Dentomaxillofac Radiol. 1997; 26:16-21.
42. González-Arriagada WA, Santos-Silva AR, Ito FA, Vargas PA, Lopes MA. Calcifications may be a frequent finding in mucoepidermoid carcinomas of the salivary glands: a clinicopathologic study. Oral Surg Oral Med Oral Pathol Oral Radiol Endod. 2011;111:482-5.
43. Coelho LOM, Ono SE, de Carvalho Neto A, Kawasaki CS, Sabóia LV, Soares MF. Massive Calcification in a Pleomorphic Adenoma: Report of an Unusual Presentation. Ear Nose Throat J. 2013;92:E6-7.